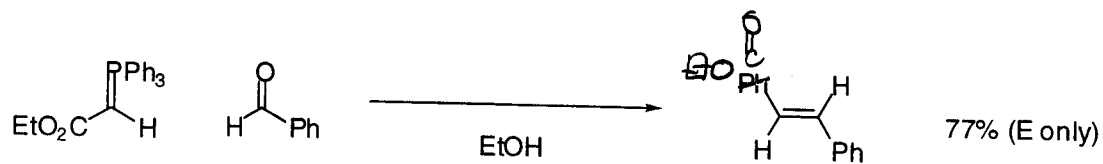
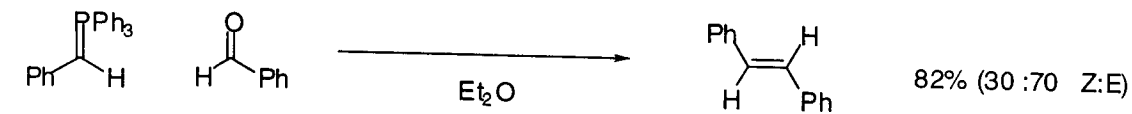
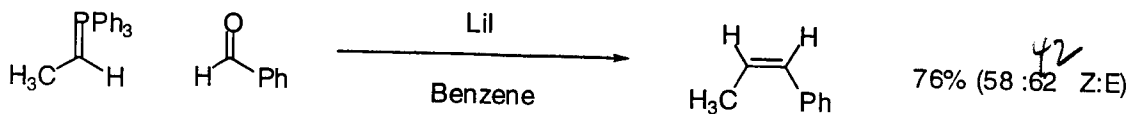
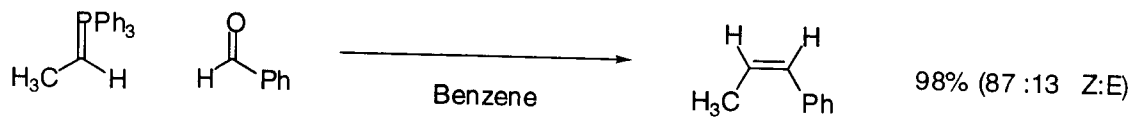


Mechanism of the Wittig Reaction

Michael Ober

08/20/02

The Wittig Reaction



Vedejs, E.; Peterson, M.J. *Advances in Carbanion Chemistry* **1996**, 2, 1-85.
Vedejs, E.; Peterson, M.J. *Topics in Stereochemistry* **1994**, 21, 1-157.
Maryanoff, B.E.; Reitz, A.B. *Chem. Rev.* **1989**, 89, 863-927.
Schlosser, M. *Topics in Stereochemistry* **1970**, 5, 1.

Original Mechanistic Ideas

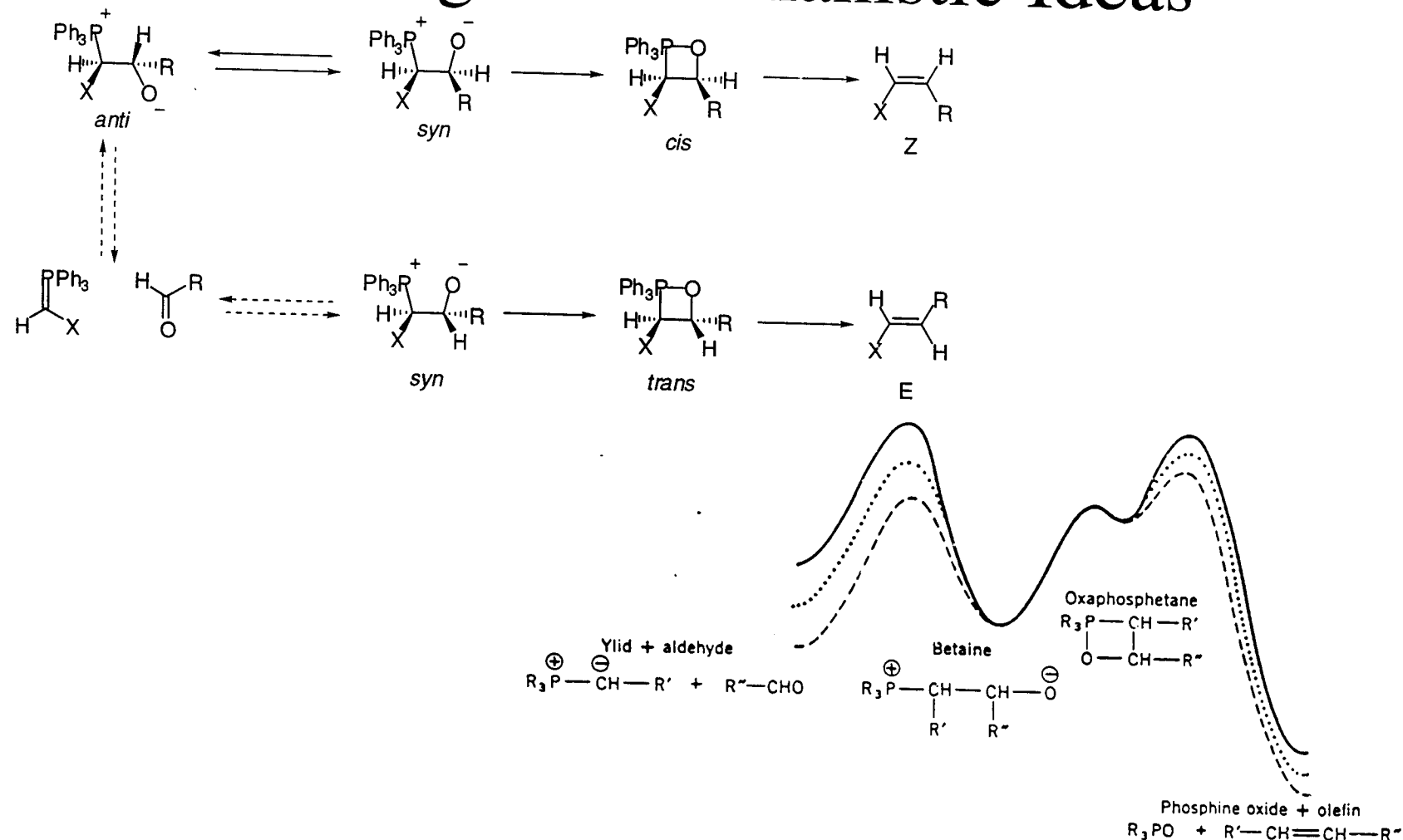
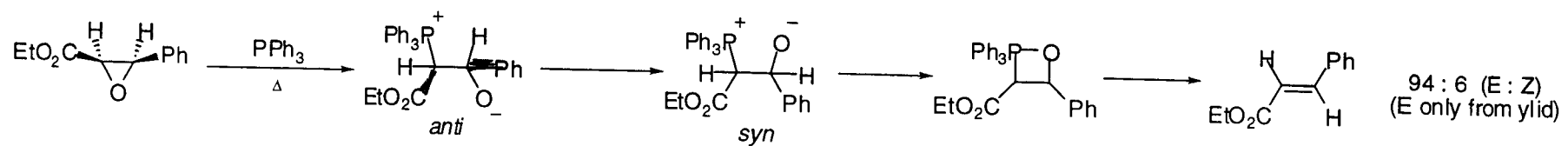
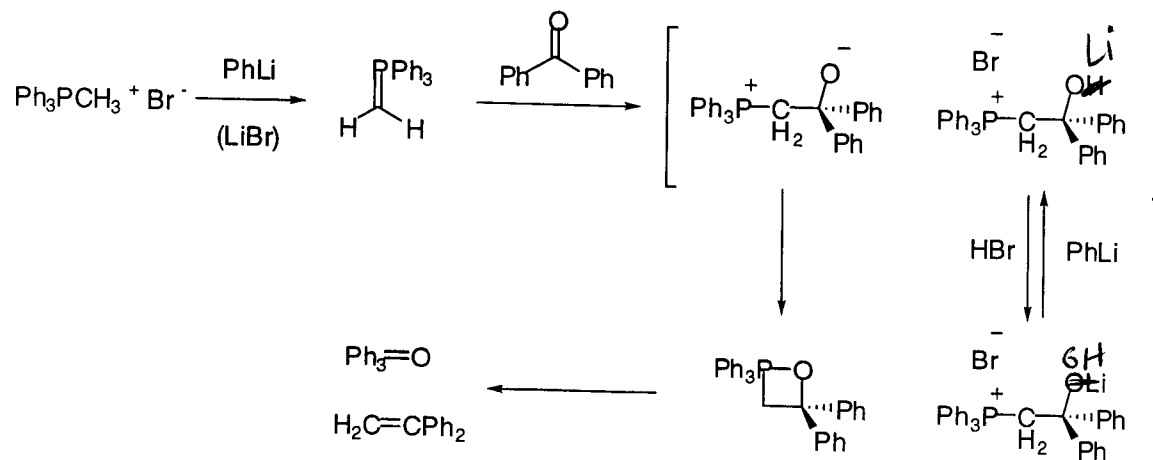


Figure 1. (Assumed) energy profile of the Wittig carbonyl olefination reaction, effected by (—) "reactive", (···) "moderated," or (----) "stable" phosphonium ylids. (In the following figures the hypothetical oxaphosphetane intermediate will be omitted, since it has no further bearing on the discussion.)

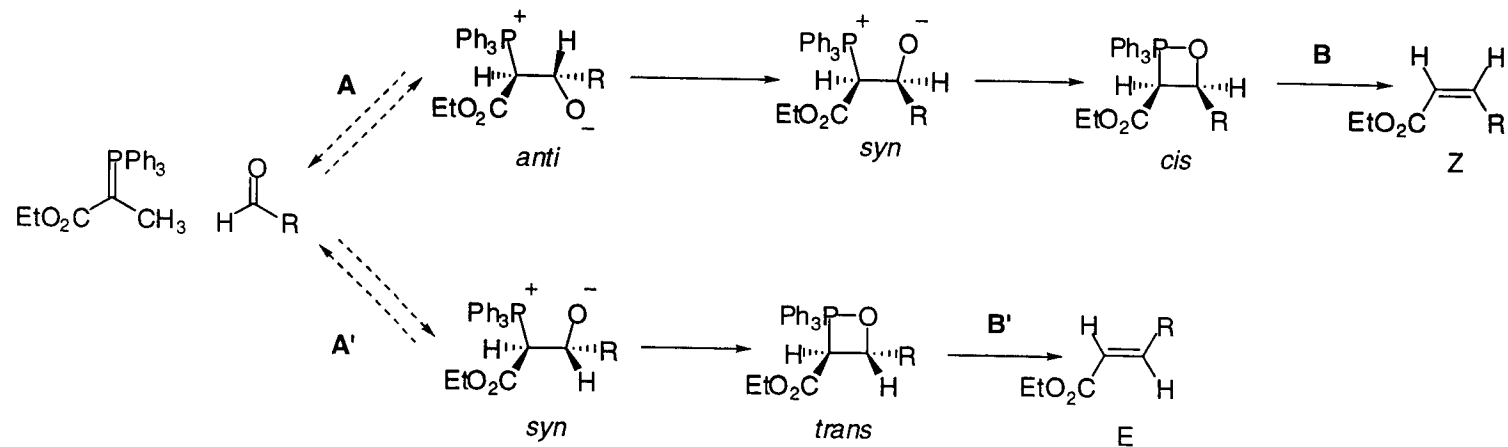
House H. O.; Jones, V. K.; Frank G.A. *J. Org. Chem.* **1964**, *29*, 3327.
Bergelson, L.D.; Shemyakin, M. M. *Angew. Chem. Int. Ed.* **1964**, *3*, 250

Origins of the Original Proposal



Wittig, G. Haag, W. *Chem. Ber.* **1955**, *88*, 1654.
Wittig, G.; Schollkopf, U. *Chem. Ber.* **1954**, *87*, 1318.

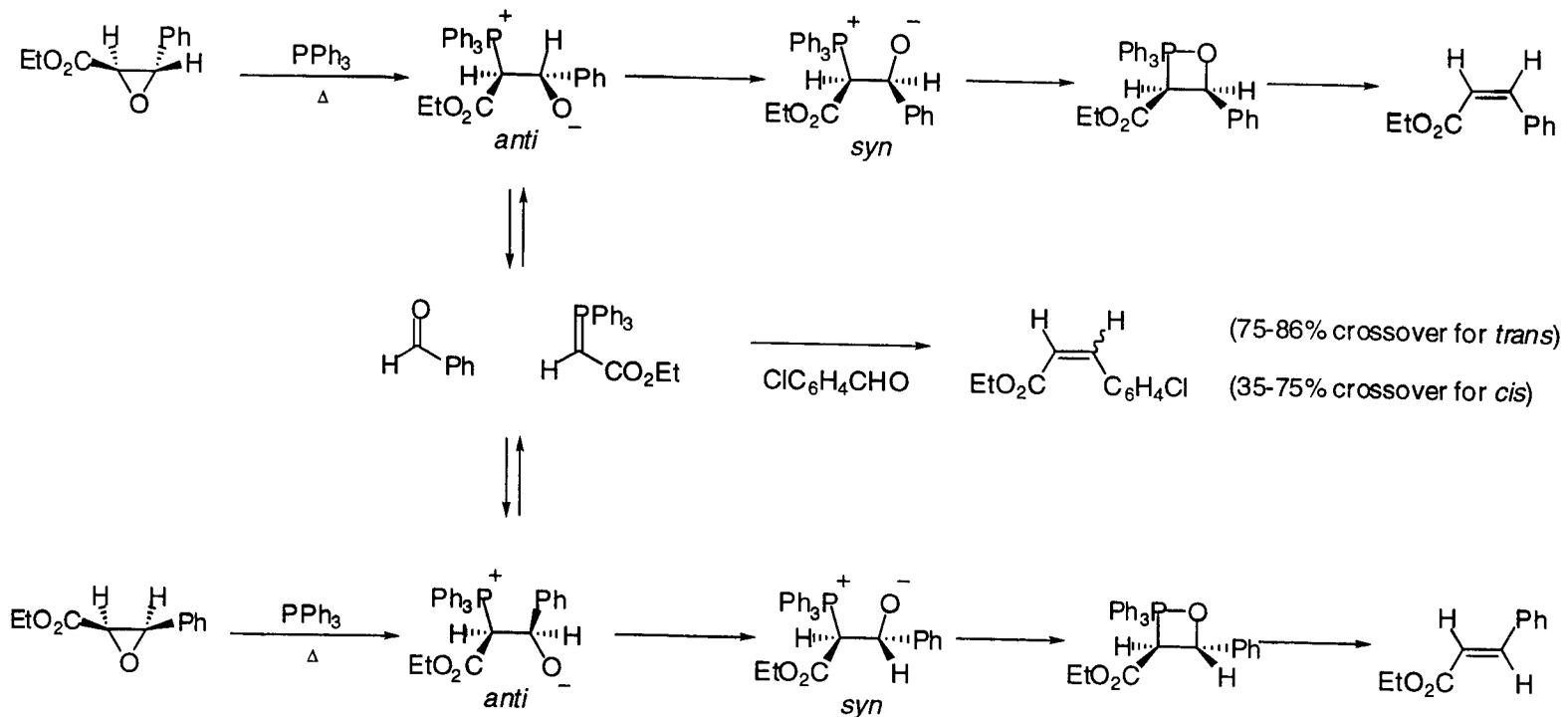
Origins of the Original Proposal II



A / A' - Stereochemical leakage due to reversibility of betaines

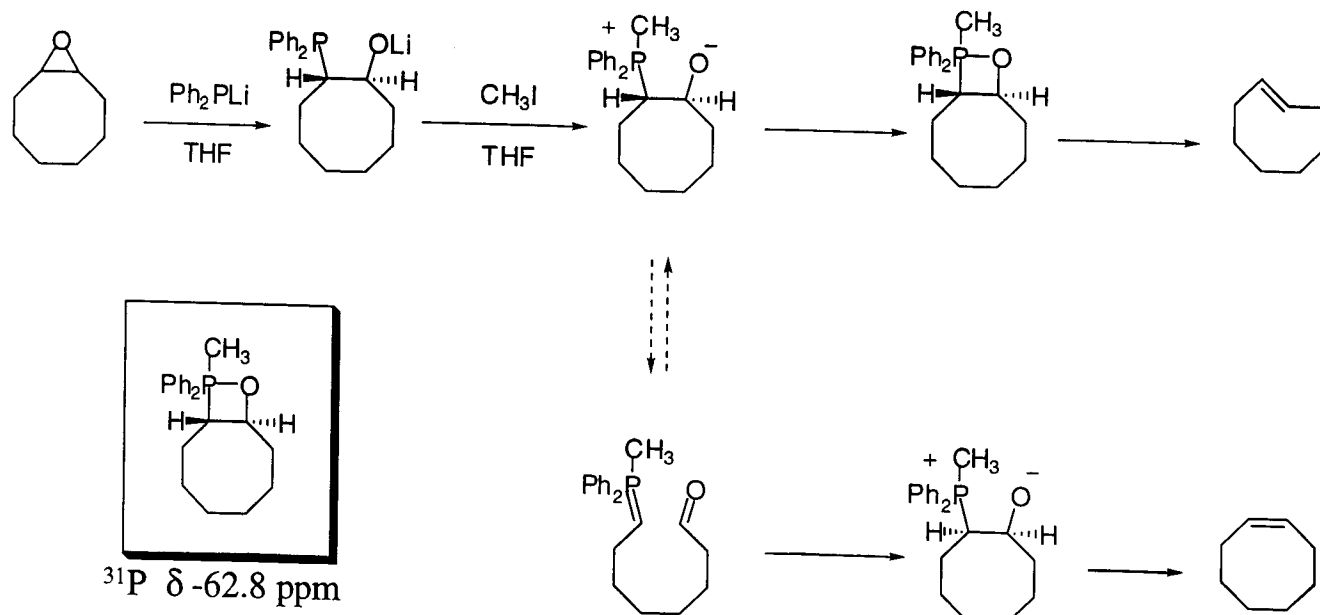
B / B' - Stereochemical leakage due to collapse of oxaphosphoranes

Reversibility of the Betaine



Speziale, A. J.; Bissing, D.E. *J. Am. Chem. Soc.* **1963**, *85*, 3878.
 Speziale, A. J.; Bissing, D.E. *J. Am. Chem. Soc.* **1965**, *87*, 2683.

An Unexpected Result



Pentacoordinate ³¹P δ -50 to -80 ppm
Phosphorous

Tetracoordinate ³¹P δ 10 to 50 ppm
phosphorous

Oxaphosphetane as an Intermediate

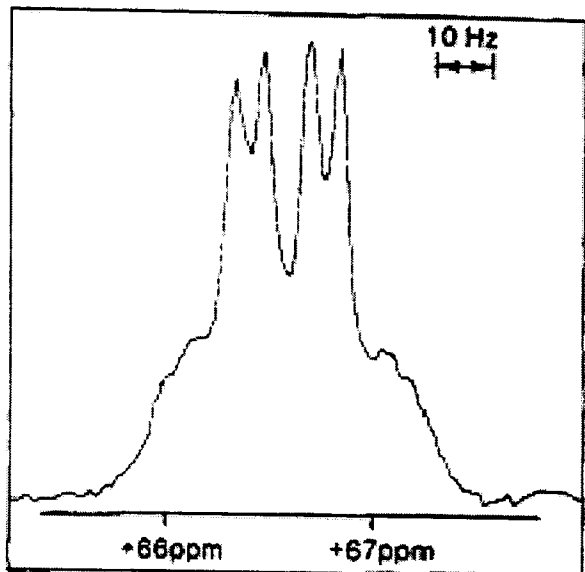
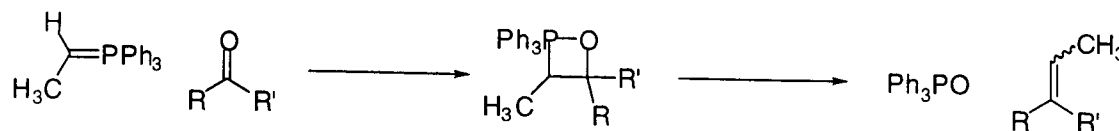
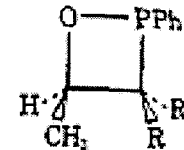


Figure 1. Nmr spectrum of the cyclohexanone-ethyldienetriphenylphosphorane adduct (-70° , THF), phenyl hydrogens decoupled.

Table I. Oxaphosphetanes from the Wittig Reaction of Ethyldienetriphenylphosphorane in THF

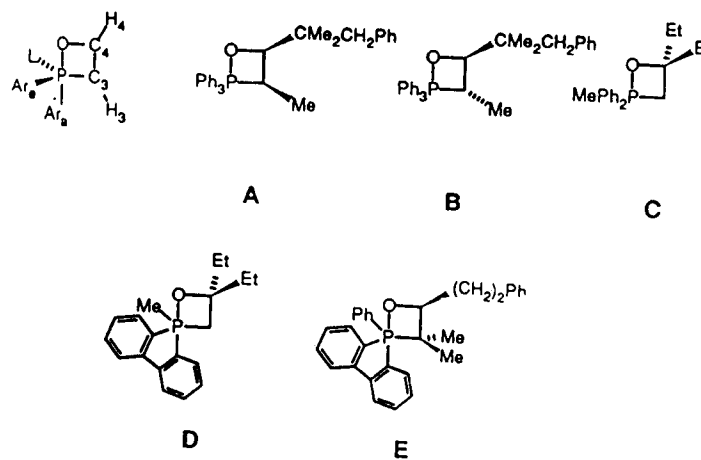
Carbonyl component	Oxaphosphetane	$\delta_{\text{H}}^{\text{ppm}}$ at -70°	Cis:trans olefin ratio
Cyclohexanone	2	+66.5	
$(\text{CH}_2)_5\text{CCHO}$	5a	64.2	99:1
$\text{C}_6\text{H}_5\text{CHO}$	6a,b	62.7	2:1
$\text{C}_6\text{H}_5\text{CH}_2\text{CH}_2\text{CHO}$	7a,b	61.9	7:3



- 5a, R = $\text{C}(\text{CH}_3)_3$; R' = H
 b, R = H; R' = $\text{C}(\text{CH}_3)_3$
 6a, R = C_6H_5 ; R' = H
 b, R = H; R' = C_6H_5
 7a, R = $\text{C}_6\text{H}_5\text{CH}_2\text{CH}_3$; R' = H
 b, R = H; R' = $\text{C}_6\text{H}_5\text{CH}_2\text{CH}_3$

Oxaphosphetanes : Solid Evidence

Table 1. NMR Data of Representative Oxaphosphetanes^{a,b}



$\delta^{31}P$	δ^1H				$\delta^{13}C$		
	$H_3(J_{HP})$	$H_4(J_{HP})$	$C_3(J_{CP}), C_4(J_{CP})$	$L(J_{CP})$	$Ar_e(J_{CP})$	$Ar_d(J_{CP})$	$C_3Me(J_{CP})$
P							
A (-62.9)	4.09(16)	3.52(6)	65.2(85), 69.9(16)	—	—	—	11.5(9)
B (-62.2)	4.56(22)	3.05(2)	59.3(85), 73.5(15)	—	—	—	13.8(9)
C (-70.8)	3.56(16)	—	60.3(83), 66.9(15)	24.4(96)	averaged:	148.8(71)	—
D ^c (-79.2)	3.93(17) 2.82(15) ^c	—	54.5(82), 67.3(16)	21.9(98)	134.3(132), X ^d (<19)	—	—
E ^e (-61.7)	—	3.44(3) ^c	67.0(88), 71.3(16)	137.6(134)	132.2(126), X ^d (<18)	17.1(5) 21.5(<1)	

Notes: ^aData taken from Refs. 42a, 53, and 69.

^b δ , ppm (J, Hz).

^cPseudorotation frozen out at -53 °C.

^dEntries marked X indicate that the assignment of quaternary aromatic carbons is uncertain and that the J value is no larger than the value given in parentheses.

^ePseudorotation frozen out; data are given for the major pseudorotamer.

Oxaphosphetanes : Solid Evidence

TABLE 4
Oxaphosphetane Crystal Structure Data^a

Entry	dP-O	dP-C	dC-C	dC-O	$\angle OPC$	$\angle PCC$	$\angle CCO$	$\angle COP$	$\angle PCCO^b$	Reference
A	1.79	1.83	1.52	1.36	75.5	88.1	100.5	94.8	8.6	34a
B	1.85	1.61	1.48	1.43	71.6	---	---	---	---	34b
C	1.83	1.78	1.51	1.43	73.6	95.4	94.9	95.9	2.9	34c
D	2.01	1.76	1.57	1.39	71.3	98.5	96.1	94.1	0.6	34d
E	1.73	1.81	1.53	1.45	77.4	89.8	95.6	95.7	9.7	34e
F	1.78	1.82	1.55	1.40	75.5	90.2	97.0	97.0	4.7	34f

(a) Distances in angstroms, angles in degrees
(b) Dihedral angle

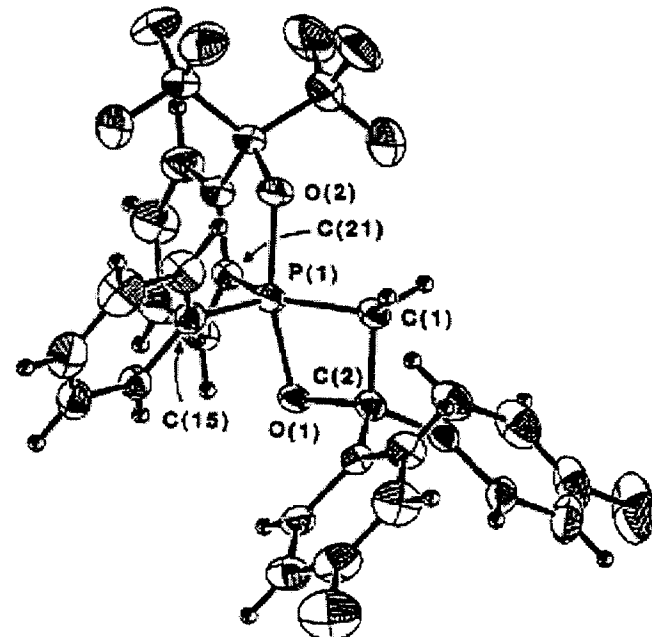
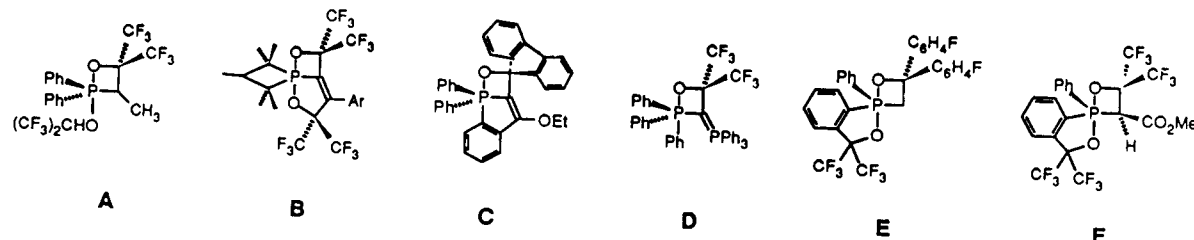


Figure 1. ORTEP drawing of 3d. Selected bond lengths (\AA) and bond angles (deg): P(1)-O(1), 1.728 (2); P(1)-O(2), 1.754 (3); P(1)-C(1), 1.808 (4); O(1)-P(1)-O(2), 163.3 (1); C(1)-P(1)-C(15), 111.8 (2); C(1)-P(1)-C(21), 136.0 (2); C(15)-P(1)-C(21), 112.1 (2); O(1)-P(1)-C(1), 77.4 (1); O(2)-P(1)-C(21), 87.4 (2).

Betaines vs. Oxaphosphetanes

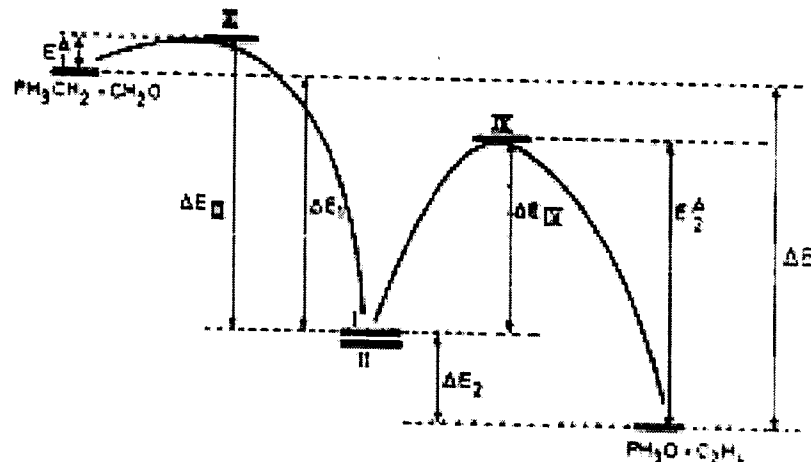


Figure 4. Energy profile for the reaction $\text{PH}_3\text{CH}_2 + \text{CH}_2\text{O} \rightarrow \text{PH}_3\text{O} + \text{C}_2\text{H}_4$. The energy differences are defined as follows: $E_1^A = E_{\text{III}} - E_{\text{PH}_3\text{CH}_2} - E_{\text{CH}_2\text{O}}$; $E_1^B = E_{\text{IV}} - E_{\text{PH}_3\text{O}} - E_{\text{C}_2\text{H}_4}$; $\Delta E_1 = E_{\text{PH}_3\text{CH}_2} + E_{\text{CH}_2\text{O}} - E_1$; $\Delta E_2 = E_{\text{PH}_3\text{O}} + E_{\text{C}_2\text{H}_4} - E_1$; $\Delta E_{\text{II}} = E_{\text{II}} - E_1$; $\Delta E_{\text{III}} = E_{\text{III}} - E_1$; $\Delta E_{\text{IV}} = E_{\text{IV}} - E_1$; $\Delta E = E_{\text{PH}_3\text{O}} + E_{\text{C}_2\text{H}_4} - E_{\text{PH}_3\text{CH}_2} - E_{\text{CH}_2\text{O}}$. Roman numbers refer to the structures I-IV defined in Figure 1 and Tables II and IV.

Table VI. Energy Differences (kcal/mol)^a

	basis					
	1 ^b	2 ^b	2 ^c	3 ^b	4 ^b	5 ^c
ΔE	-16.2	-40.5	-38.8	-49.6	-43.7	-48.3
ΔE_1	58.3	32.4	31.2	35.7	31.3	34.0
ΔE_2	42.0	-8.1	-7.6	-13.9	-12.4	-14.3
ΔE_{II}	1.9		2.8			-0.08
ΔE_{III}	61.4		27.0			39.0
ΔE_{IV}	67.0		24.0			24.4
E_1^A	3.1		-4.2			5.0
E_1^B	25.0		31.6			38.7

^a For definition see Figure 4. ^b The geometry calculated with basis set 1 has been used. ^c The geometry calculated with basis set 2 has been used.

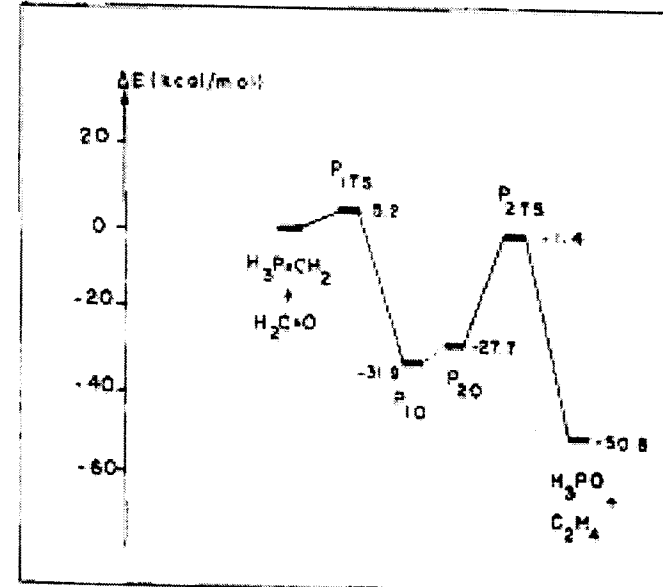
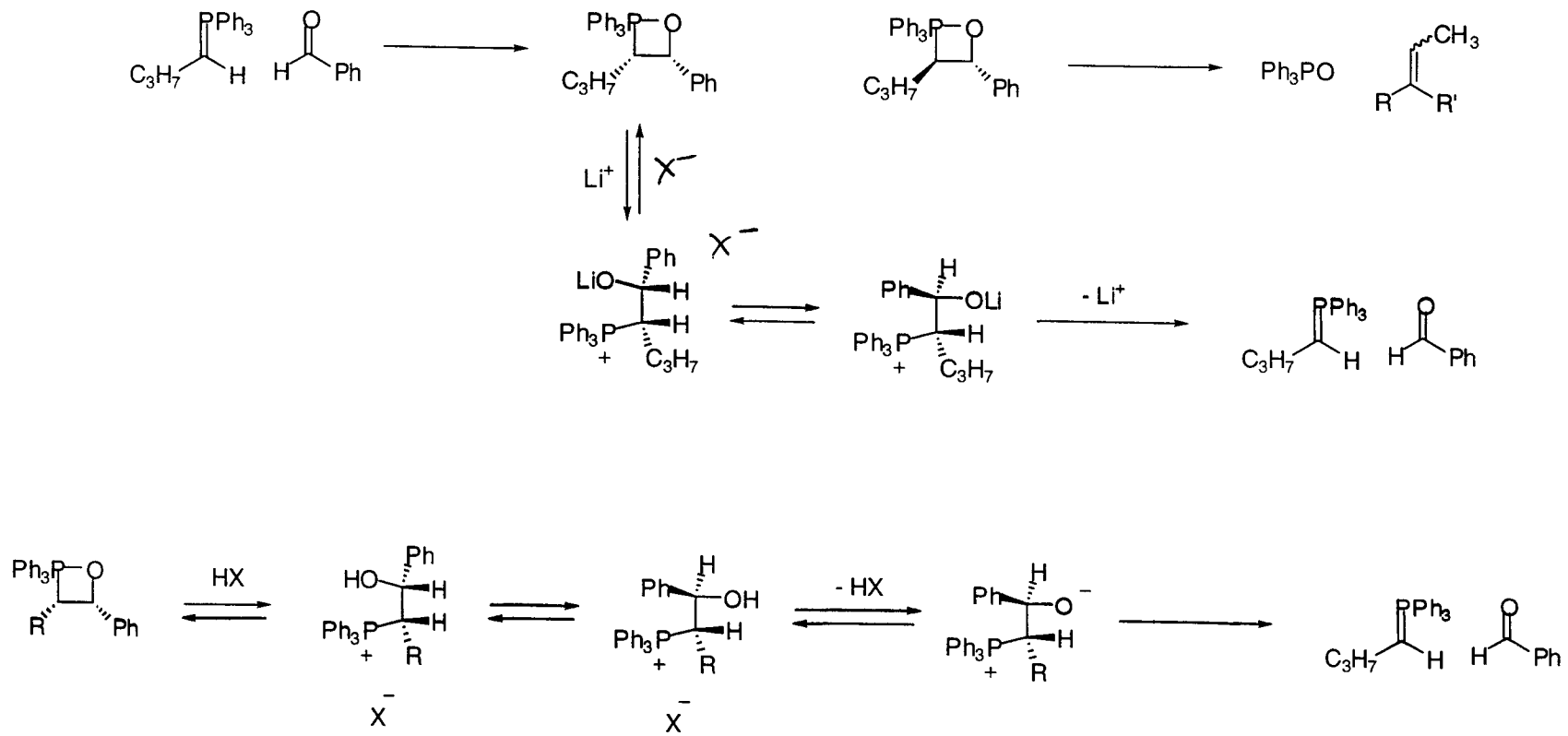


Figure 1. Energy profile for the Wittig reaction with phosphonium ylide. The energies are given for calculations at the 4-31G**/4-31G* level (1 kcal/mol = 4.18 kJ/mol).

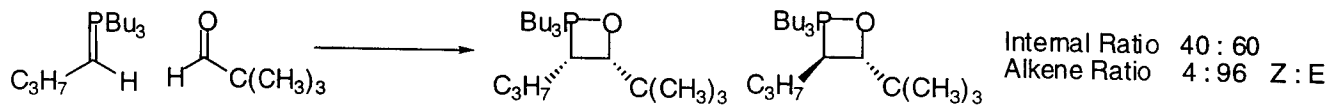
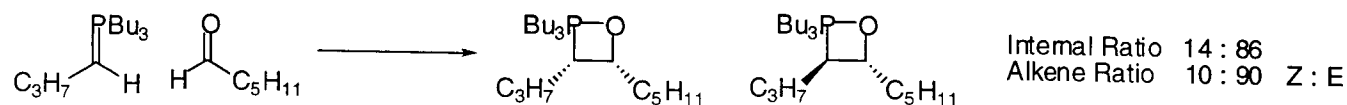
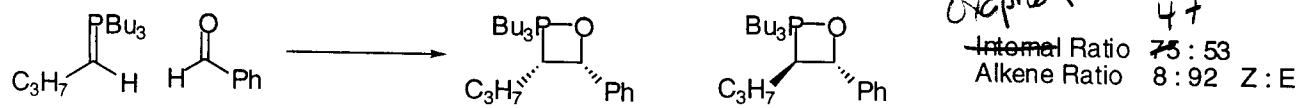
Activation energy to form betaine ~20-32 kcal/mol

Oxaphosphetane Reversibility



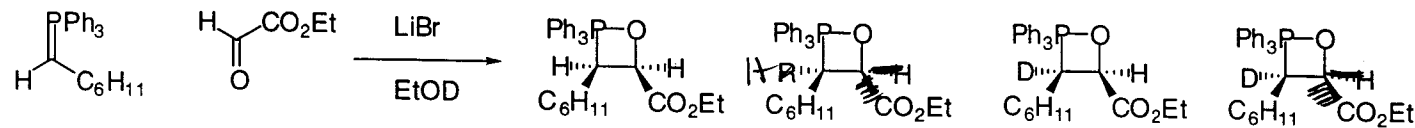
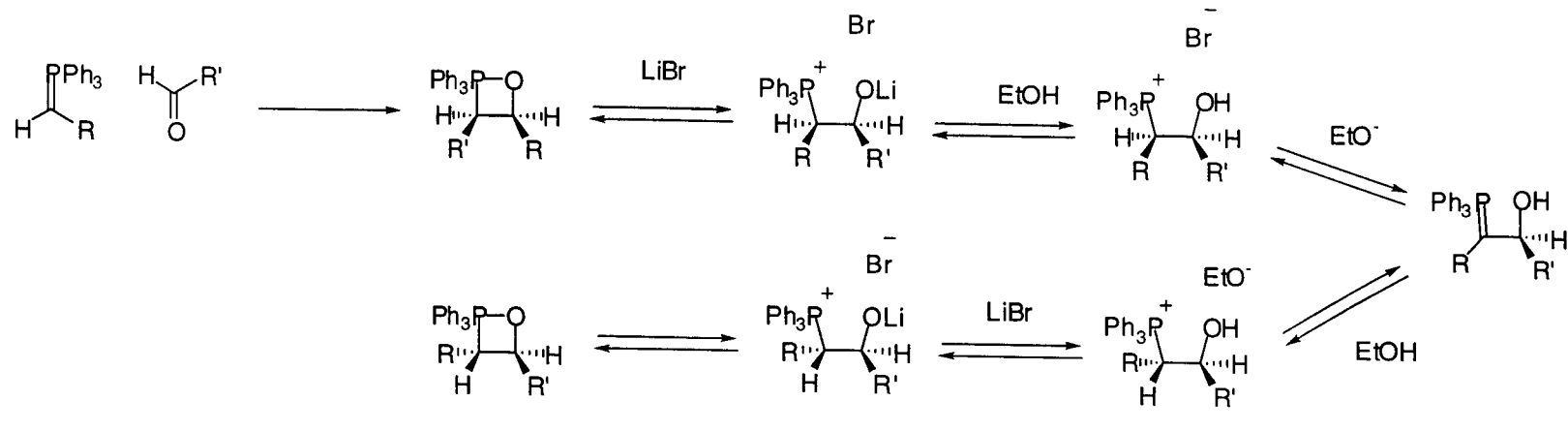
Vedejs, E.; Meier, G.P.; Snoble, K.A. *J. Am. Chem. Soc.* **1981**, *103*, 2823.
 Reitz, A.B.; Mutter, M.S.; Maryanoff, B.E. *J. Am. Chem. Soc.* **1984**, *106*, 1873.

Oxaphosphatane Reversibility II



Maryanoff, B.E. et al *J. Am. Chem. Soc.* **1986**, *108*, 7664.
 Vedejs, E.; Fleck, T. J. *J. Am. Chem. Soc.* **1989**, *111*, 5861.
 13

Oxaphosphetane Reversibility III



Anderson, R.J.; Henrick, C.A. *J. am. Chem. Soc.* **1975**, *97*, 4327.
Bestman, H.J.; Stransky, W. *Pure & Appl. Chem.* **1979**, *51*, 515.

Summary of the Stereo-equilibration of Oxaphosphetanes

-
1. Lithium-free Wittig reactions proceed without significant reversal, except for the $\text{Et}_3\text{P}=\text{CHCH}_3$, or $\text{Bu}_3\text{P}=\text{CHC}_3\text{H}_7$, with tertiary or aromatic ~~halides~~ *aldehydes*
 2. Intermediates from ~~yildes~~ and aliphatic aldehydes do not undergo reversal
 3. Significant reversal occurs only for precursors of (Z)-alkenes at low temperatures
 4. Deliberate betaine generation maximizes the risk of reversal. The risk is highest for betaines corresponding to ArCHO
 5. The risk of reversal is highest for ArCHO in the presence of lithium ion, in protic solvents and at high temperatures

Rate Profiles for the Wittig Reaction

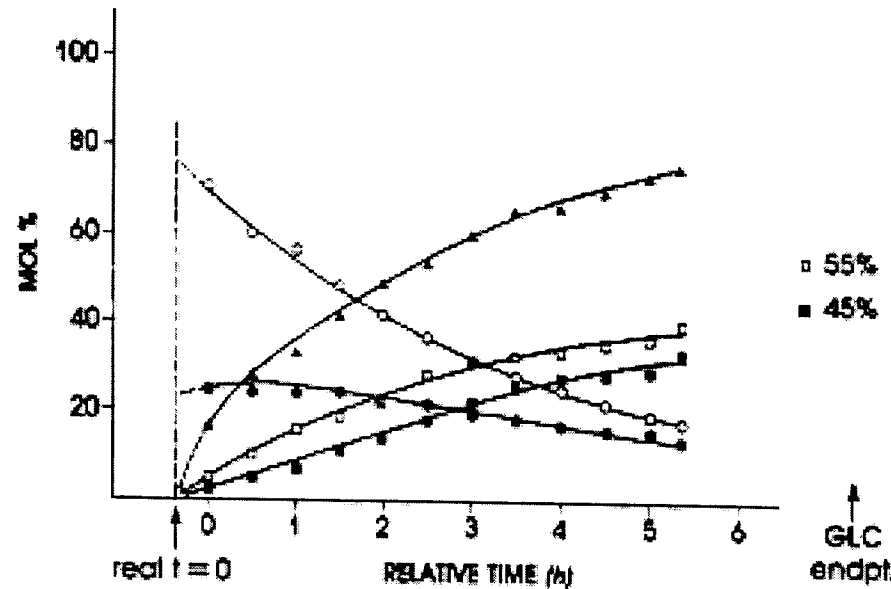
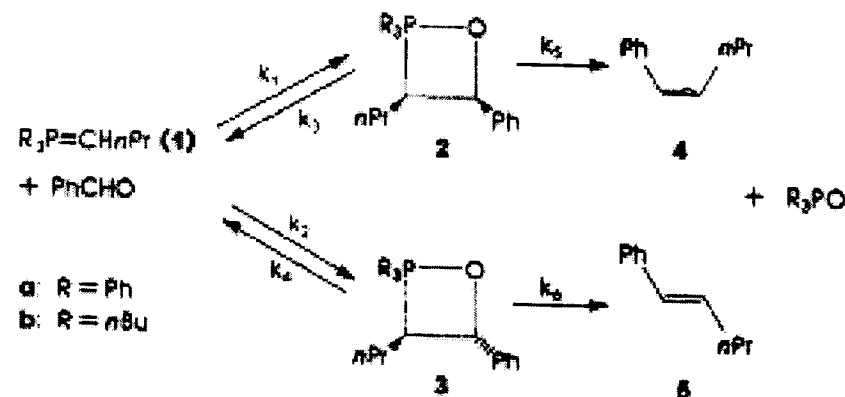


Figure 1. Kinetic plot for the reaction of **1a** and benzaldehyde (1:1 molar ratio), 0.36 M in THF- d_6 at -30°C , derived from ^{31}P - ^1H NMR data. (Broad-band proton decoupling in the ^{31}P data collection was not used to avoid differential heating.) The dotted lines indicate extrapolation. Only every third data point is displayed. Proton NMR and ^{31}P NMR data were quantitated absolutely by using external references in glass capillaries: trimethyl orthobenzoate and trimethyl phosphite, respectively. Legend: (▲) triphenylphosphine oxide, (○) **2a**, (●) **3a** [from ^{31}P NMR]; (□) **4**, (■) **5** [from ^1H NMR].

Scheme 1



$$k_1 / k_2 = 3.50$$

$$k_3 = 13.9 \pm 2.7$$

$$k_4 = 0.9 \pm 1.3$$

$$k_5 = 4.78 \pm 0.04$$

$$k_6 = 7.90 \pm 0.09$$

$$\frac{k_1 / k_3}{k_2 / k_4}$$

$$\frac{k_1 / k_3}{k_2 / k_4} \frac{k_1 / k_4}{k_2 / k_3}$$

Concentration Effects on the Reaction

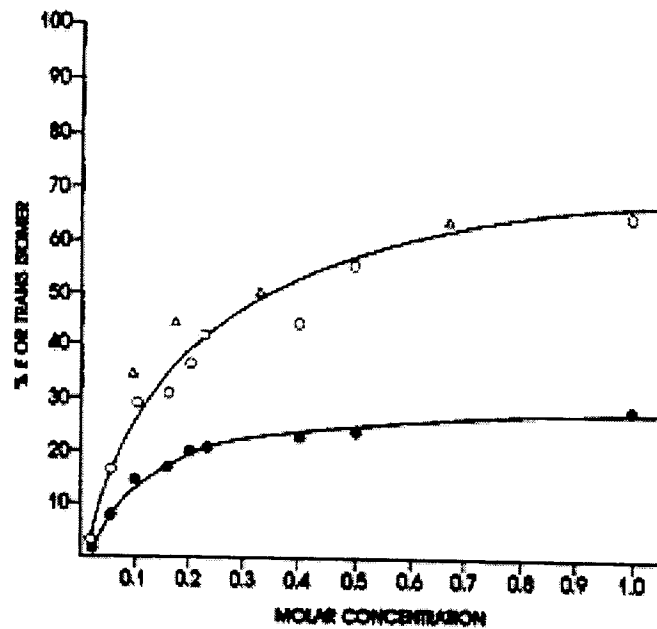


Figure 1. Plot of the relative levels of *trans*-oxaphosphetane and (*E*)-alkene vs. concentration for the reaction of ylide 1 with benzaldehyde in the presence of LiBr in THF. The lines connecting the data points are meant to serve as an aid to the reader: (●) percent 3a determined by ^{31}P NMR at -40°C , (○) percent 5a from NMR experiments determined by GLC, and (△) percent 6a from room-temperature experiments determined by GLC.

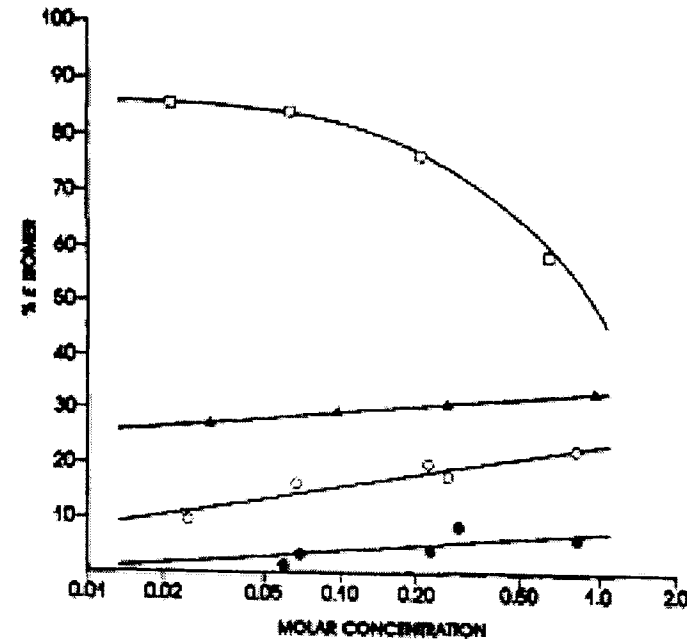
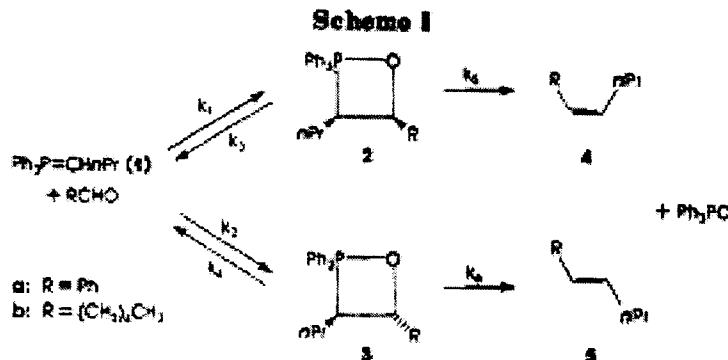
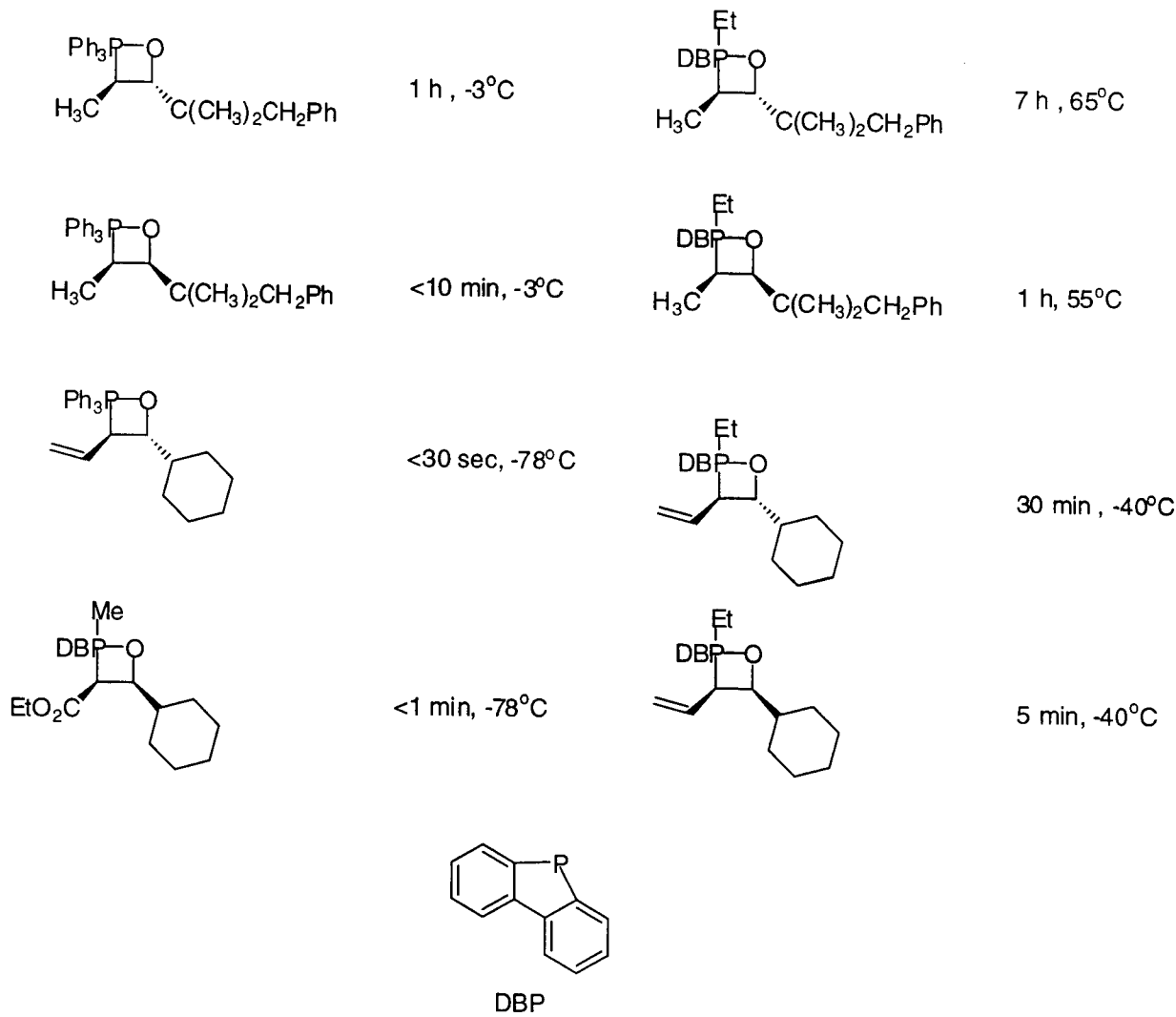
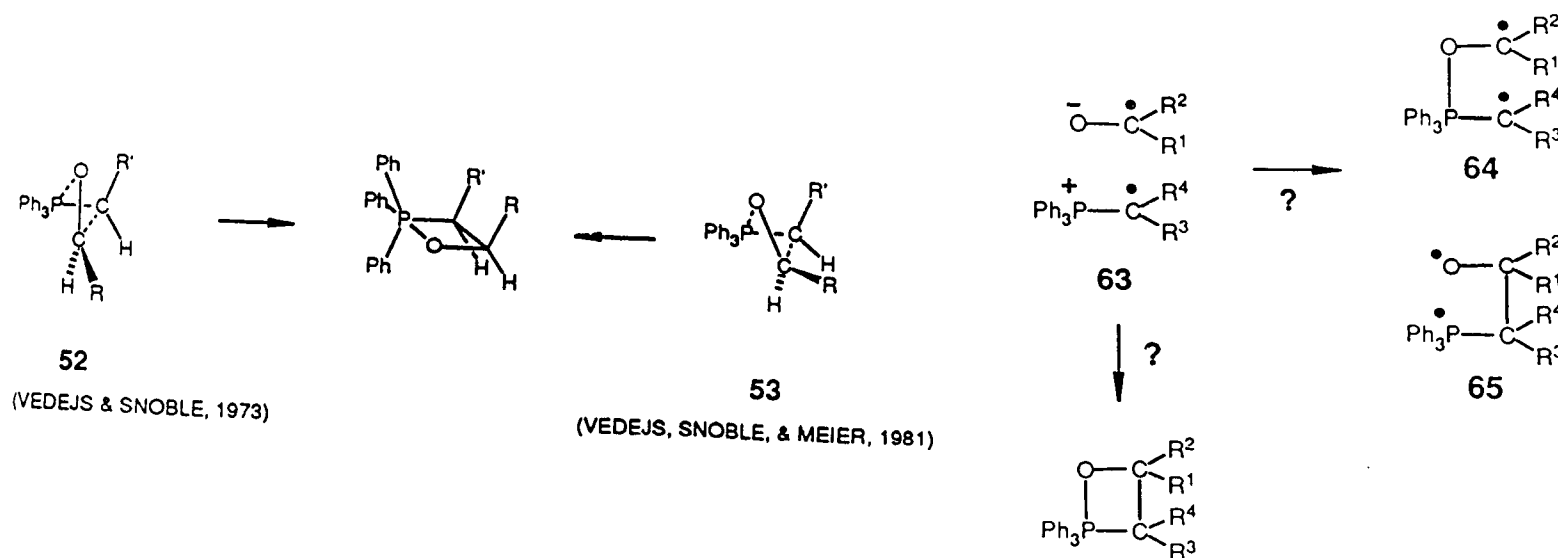
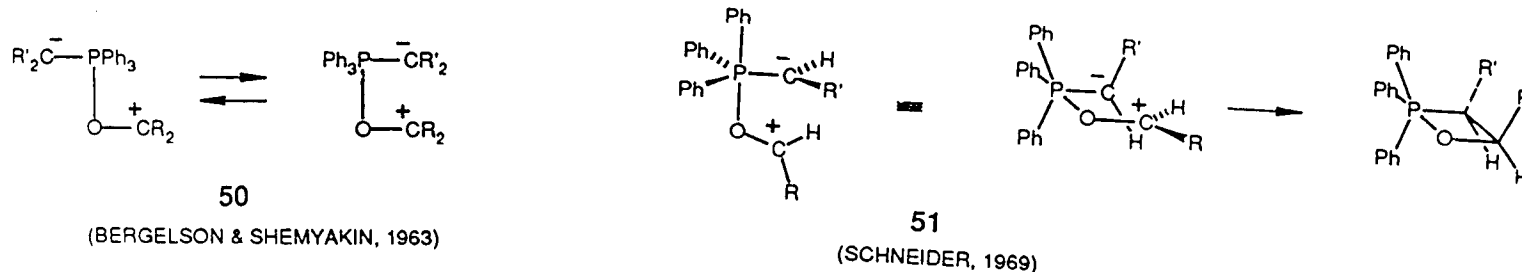


Figure 3. Semi-log plot of the relative levels of (*E*)-alkene determined by GLC vs. concentration for reactions of ylide 1 with benzaldehyde or hexanal. The straight lines defined by the open circles and closed triangles are derived from least-squares analysis ($r^2 = 0.92$ or better); the other two lines were drawn as an aid to the reader: (○) percent 5b from 1 and hexanal in THF (LiHMDS), (●) percent 5a from 1 and benzaldehyde in THF (NaHMDS), (▲) percent 5a from 1 and benzaldehyde in Me_2SO (LiHMDS), and (□) percent 5a from 1 and benzaldehyde in toluene (LiHMDS).

Decomposition of Oxaphosphetanes



Revamped Mechanistic Proposals



Vedejs, E.; Snoble, K.A. *J. Am. Chem. Soc.* **1973**, *95*, 5778.¹⁹

Vedejs, E.; Meier, G.P.; Snoble, K.A. *J. Am. Chem. Soc.* **1981**, *103*, 2823.

Mechanistic Insights

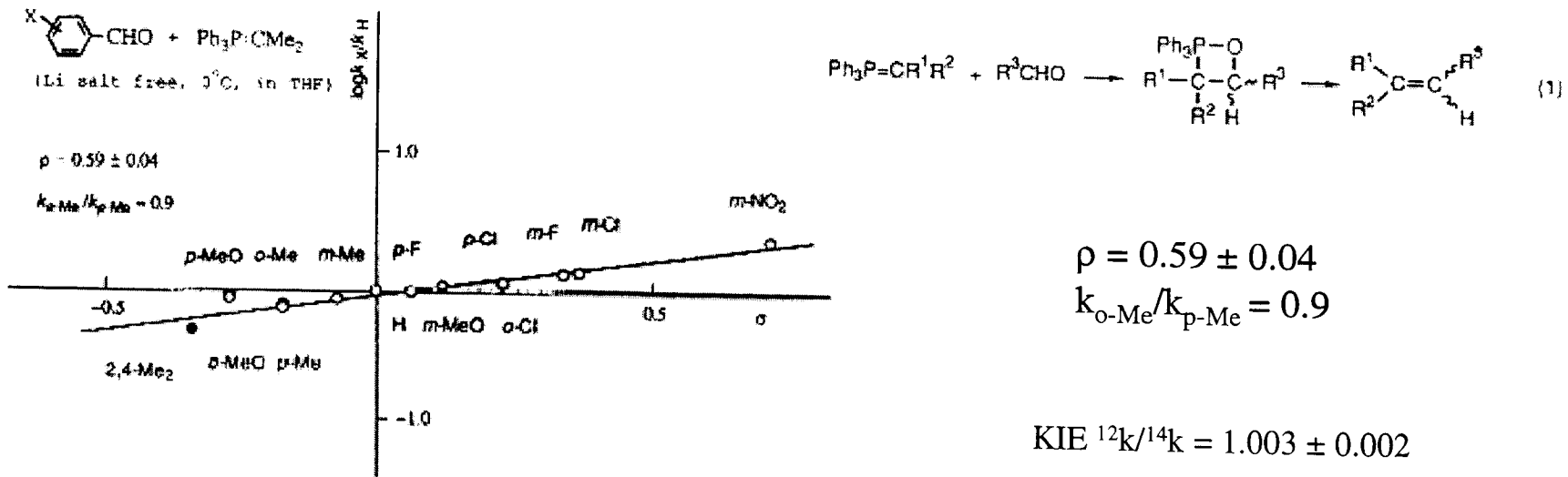
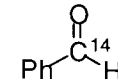


Figure 1. Substituent effects in the oxaphosphetane formation between benzaldehyde and 1a.

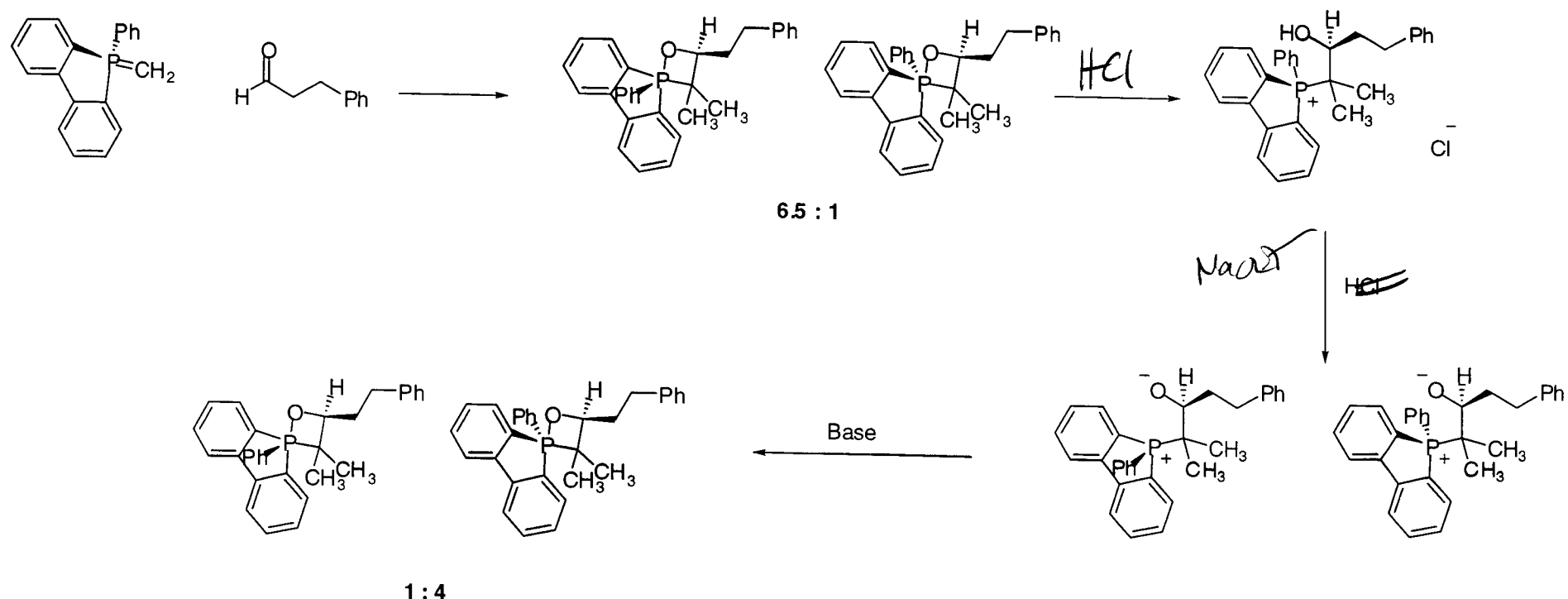


Solvent	DMF	CH_2Cl_2	C_6H_6	CH_3CN	CH_3OH	CCl_4	$t\text{-C}_5\text{H}_{11}\text{OH}$
Rate ($\times 10^4$)	6.1	9.8	20.2	55.0	58.0	351	1567
ΔH	11.3	13.2	10.0	10.0	16.2	8.9	10.9
ΔS	-35.3	-26.5	-37.0	-35.1	-14.3	-35.1	-25.4

From Review

Yamataka H. et al *J. Org. Chem.* **1988**, *53*, 3877.
Yamataka H. et al *Tetrahedron Lett.* **1989**, *30*, 7187.
²⁰

Betaine as an Intermediate?



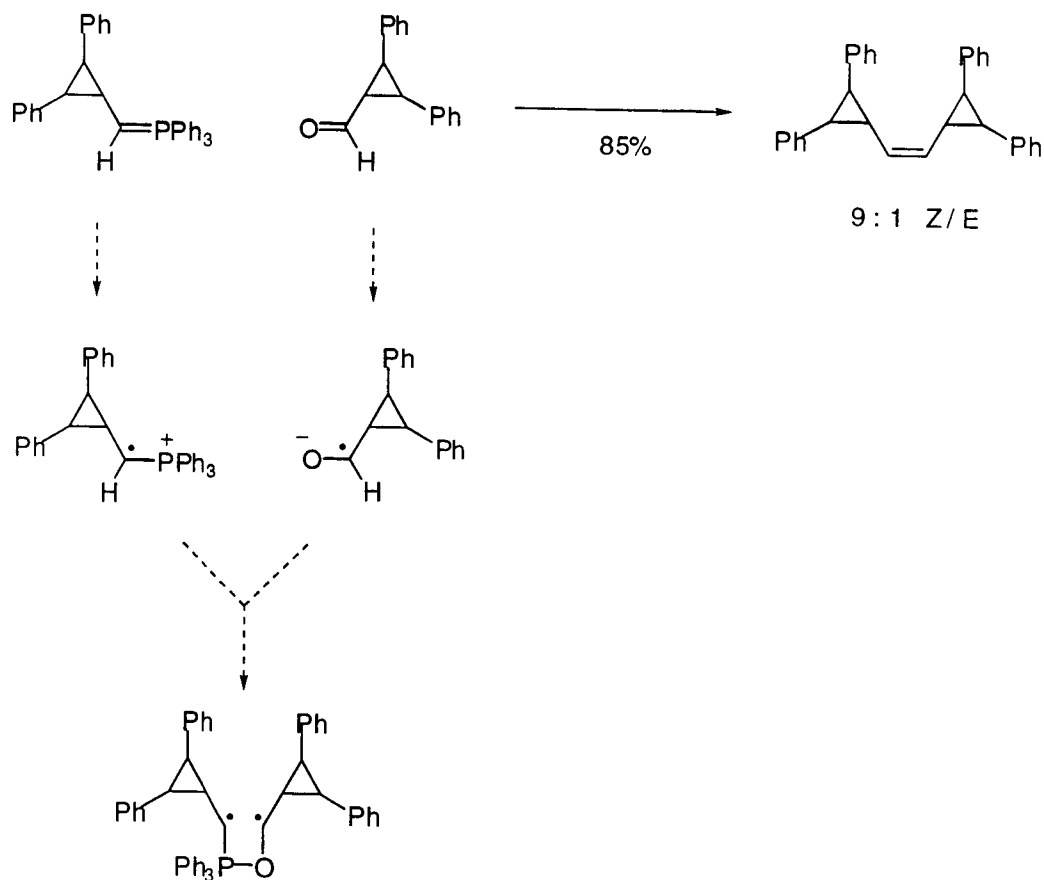
21

Vedejs, E.; Marth, C.F. *J. Am. Chem. Soc.* **1990**, *112*, 3905

The SET Mechanism



$\text{X} = \text{Halide, Selenide, or epoxide}$



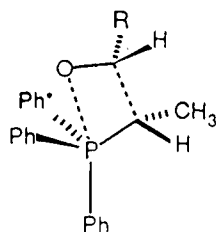
Cycloaddition Mechanism

cis SELECTIVE GEOMETRIES:

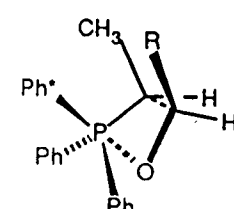
EARLY TRANSITION STATE;

PLANAR 4-CENTER INTERACTION;

SIDE VIEW:



TOP VIEW:

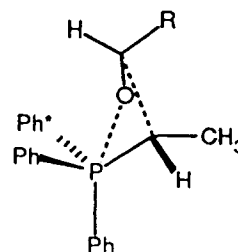


126

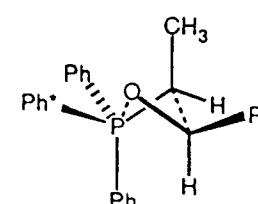
EARLY TRANSITION STATE;

PUCKERED GEOMETRY;

SIDE VIEW:



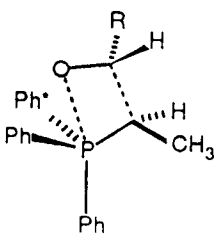
TOP VIEW:



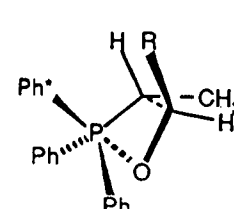
127

trans SELECTIVE GEOMETRIES:

SIDE VIEW:

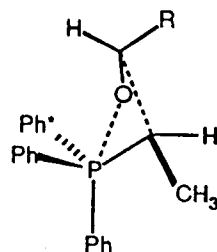


TOP VIEW:

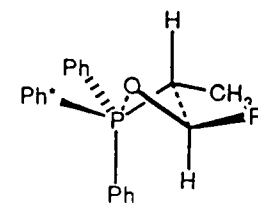


128

PUCKERED GEOMETRY;
SIDE VIEW:



TOP VIEW:

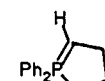


129

23

Experimental Support

Table 5. Kinetic Selectivity for *cis*-Oxaphosphetane

		a	b	c		118		a	b
	<i>R'</i> =	<i>CO₂Et</i>	<i>CO₂Et</i>	<i>CH=CH₂</i>			<i>R'</i> =	<i>CH₃</i>	<i>C₃H₇</i>
117	<i>L</i> =	<i>Ph</i>	<i>Me</i>	<i>Ph</i>			<i>L</i> =	<i>Et</i>	<i>n-Bu</i>
	1°	4%	19%	45%			1°	33%	14%
	3°	5%	22%	55%			3°	70%	40%
	Ref.	(32a)	(32a)	(80)			Ref.	(53)	(63)
119	<i>L</i> =	a <i>Et</i>	b <i>i-Pr</i>	c <i>t-Bu</i>	d <i>Ph</i>	120	<i>L</i> =	a <i>Et</i>	b <i>i-Pr</i>
	1°	30%	18%	95%	94%		1°	35%	74%
	3°	85%	50%	99%	99%		3°	57%	74%
	Ref.	(53)	(53)	(53)	(53)		Ref.	(53)	(53)
121			122			123			
	1°	14%		1°	>98%		1°	81%	
	3°	50%		3°	>98%		3°	88%	
	Ref.	(55)		Ref.	(53)		Ref.	(80a)	
124	<i>L</i> =	a <i>Ph</i>	b <i>NMe₂</i>	c <i>t-Bu</i>	d <i>Et</i>	125			
	1°	50%	82%	32%	5%				
	3°	80%	96%	75%	10%				
	Ref.	(53)	(53)	(80a)	(68)				

Note: ^a 1° = *RCH₂CHO*; 3° = *RC(Me)₂CHO*.

Computational Support

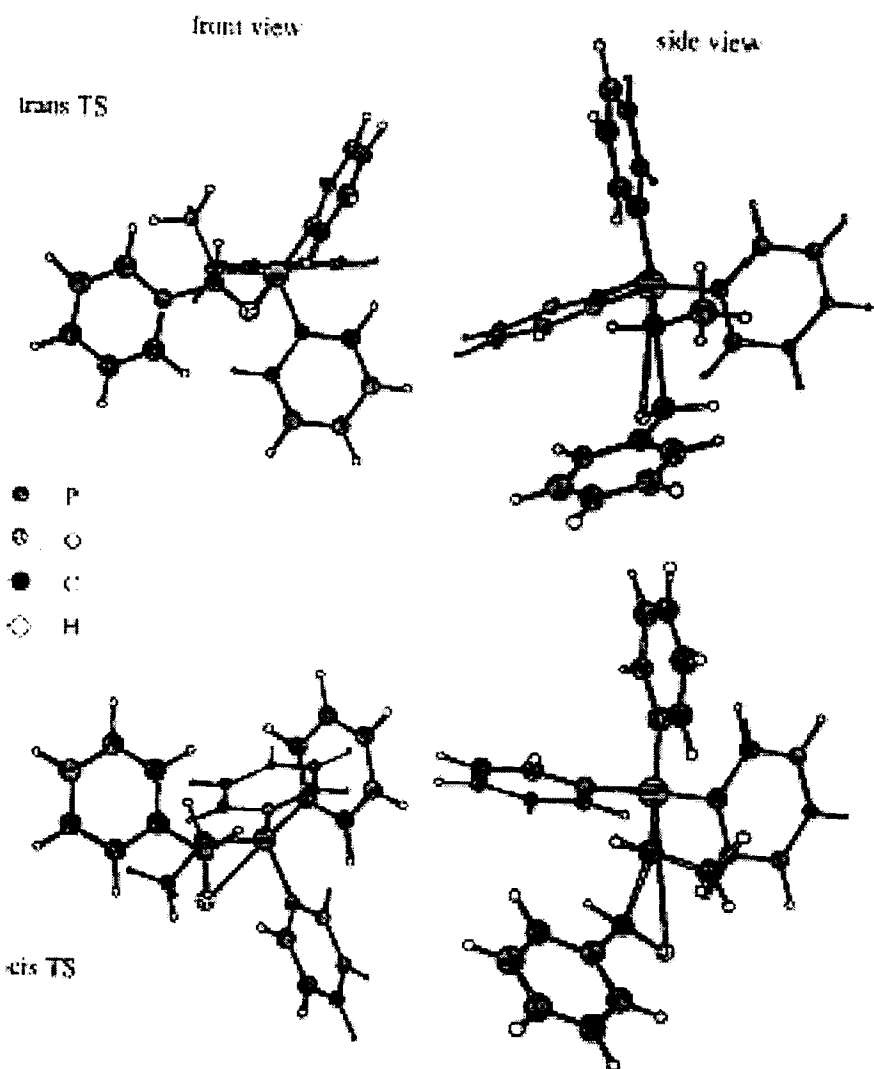


Figure 1. The trans and cis TS structures for reaction 8 calculated at B3LYP/6-31G⁺.

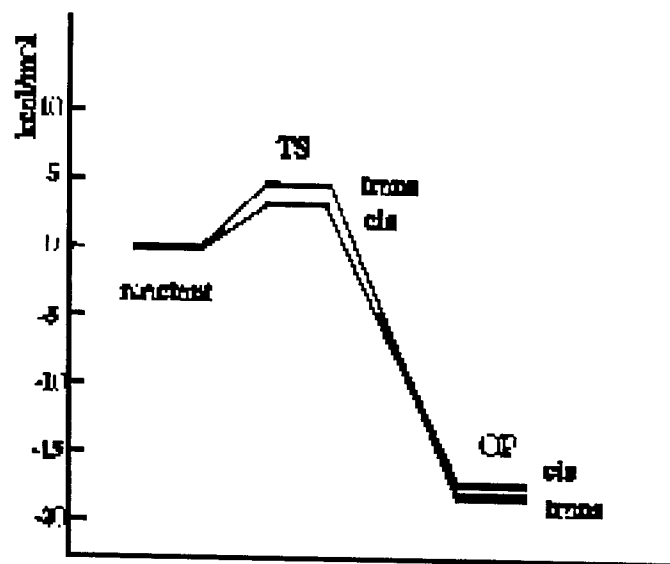
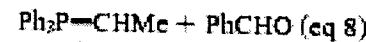


Figure 2. Reaction energy profile of reaction 8 calculated at B3LYP/6-31G⁺.



		$R_{\text{C}-\text{C}}$	$R_{\text{P}-\text{O}}$	ϕ	
HF/3-21G ⁺	trans	2.132	3.213	10.5	
	cis	2.104	3.692	87.3	
	trans	2.050	3.103	29.2	
	cis	1.977	3.660	86.5	
B3LYP/6-31G ⁺		ΔE^t	$\delta\Delta E^{t,0}$	ΔH^t	$\delta\Delta H^{t,0}$
	trans	7.3	1.7	8.5	1.5
	cis	5.6		7.0	
	trans	4.7	1.4		
	cis	3.3			

Computational Support

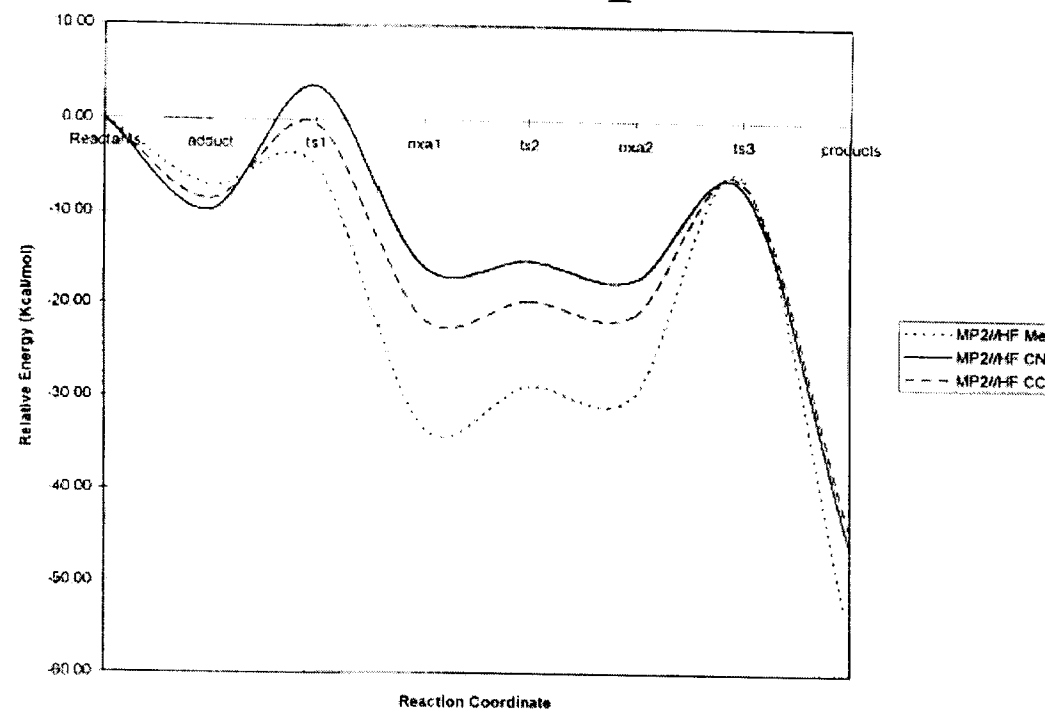
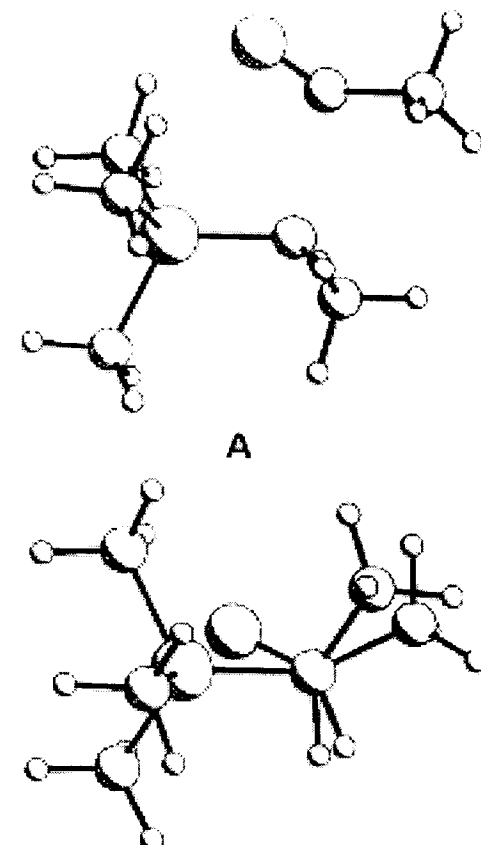


TABLE 1 MP2//HF Relative Energies (in Kcal/mol) of the Reactions of Unstabilized, Semistabilized, and Stabilized Ylides with Acetaldehyde^a

Ylide	Isomer	Adduct	Barrier ^b	oxa1	Barrier ^b	oxa2	Barrier ^b	Prod- ucts
Me	cis	-7.14	2.22(-4.92)	-33.32	4.52(-28.80)	-29.80	23.72(-6.09)	-55.30
	trans	-4.48	-2.44(-6.92)	-34.94	4.89(-30.05)	-31.15	24.30(-6.85)	-56.99
CCH	cis	-8.65	8.22(-0.44)	-21.51	1.89(-19.62)	-21.10	14.57(-6.53)	-44.16
	trans	-8.12	6.15(-1.97)	-22.45	3.17(-19.28)	-21.62	15.08(-6.53)	-44.13
CN	cis	-9.76	13.42(3.66)	-15.88	0.69(-15.19)	-17.21	10.04(-7.17)	-46.02
	trans	-9.69	12.03(2.34)	-16.72	-0.58(-17.30)	-17.44	10.14(-7.29)	-46.04

^aAll calculations were carried out using the 6-31G* basis set and ZPE corrections at the HF/6-31G* level.

^bNumbers in parentheses are the relative energies of the transition states with respect to the reactants.



Summary and Conclusions

- The new understanding of the Wittig reaction allows for a better method of predictability of stereochemistry for the reaction.
- The discovery of oxaphosphetanes as intermediates has led to a new understanding of the Wittig reaction, but some questions still remain.
- Use of computational methods does give insight into the mechanism of the cycloaddition, but does not give the entire picture.
- Experimentally, the mechanism of semi-stabilized and stabilized ylides is at the moment not attainable due the inability to view the corresponding oxaphosphetanes under applicable conditions

